Molecular Therapy
Original Article

Viral Vector Reprogramming of Adult Resident Striatal Oligodendrocytes into Functional Neurons

Marc S. Weinberg,[1] Hugh E. Criswell,[2,4] Sara K. Powell,[1] Aadra P. Bhatt,[3] and Thomas J. McCown[1,4]

[1]UNC Gene Therapy Center, University of North Carolina at Chapel Hill, Chapel Hill, NC 27599, USA; [2]Bowles Center for Alcohol Studies, University of North Carolina at Chapel Hill, Chapel Hill, NC 27599, USA; [3]Department of Chemistry, University of North Carolina at Chapel Hill, Chapel Hill, NC 27599, USA; [4]Department of Psychiatry, University of North Carolina at Chapel Hill, Chapel Hill, NC 27599, USA

Recent advances suggest that in vivo reprogramming of endogenous cell populations provides a viable alternative for neuron replacement. Astrocytes and oligodendrocyte precursor cells can be induced to transdifferentiate into neurons in the CNS, but, in these instances, reprogramming requires either transgenic mice or retroviral-mediated gene expression. We developed a microRNA (miRNA)-GFP construct that in vitro significantly reduced the expression of polypyrimidine tract-binding protein, and, subsequently, we packaged this construct in a novel oligodendrocyte preferring adeno-associated virus vector. Ten days after rat striatal transduction, the vast majority of the GFP-positive cells were oligodendrocytes, but 6 weeks to 6 months later, the majority of GFP-positive cells exhibited neuronal morphology and co-localized with the neuronal marker NeuN. Patch-clamp studies on striatal slices established that the GFP-positive cells exhibited electrophysiological properties indicative of mature neurons, such as spontaneous action potentials and spontaneous inhibitory postsynaptic currents. Also, 3 months after striatal vector administration, GFP-positive terminals in the ipsilateral globus pallidus or substantia nigra retrogradely transported fluorescent beads back to GFP-positive striatal cell bodies, indicating the presence of functional presynaptic terminals. Thus, this viral vector approach provides a potential means to harness resident oligodendrocytes as an endogenous source for in vivo neuronal replacement.

INTRODUCTION

The rapidly expanding knowledge of differentiation factors has provided a basis for the emerging ability to reprogram resident cells initially in vitro and subsequently in vivo.[1] For example, after cortical injury, retroviral-mediated expression of NeuroD1 reprogrammed reactive astrocytes into NeuN-positive cells that fired action potentials and received synaptic input.[2] Similarly, astrocytes have been converted into neurons in transgenic mice that expressed three conversion factors, Asc11, Brn2a, and Myt11,[3] while after injury NG2/olig2-positive cells could be transdifferentiated into neurons by the expression of SOX2 and Asc11.[4] These studies clearly established that at least in the context of injury, astrocytes and oligodendrocyte precursor cells (OPCs) can be induced to transdifferentiate into neurons in the CNS. However, these proofs of principle involved either transgenic mice or retroviral-mediated gene expression where, in the case of retroviral vectors, the potential for insertional mutagenesis precludes clinical consideration.

Given this demonstrated potential to reprogram cells to neurons in the CNS, oligodendrocytes provide an excellent endogenous target cell population. Oligodendrocytes and OPCs comprise a substantial population in the CNS, and in many neurological disorders, the OPC population increases in areas of neuropathology. For example, animal studies have shown a significant increase in resident OPCs in models of amyotrophic lateral sclerosis,[5] temporal lobe epileptogenesis,[6] and intracerebral stroke.[7] More importantly, a significant increase in OPCs has been found in clinical samples from both amyotrophic lateral sclerosis (ALS) patients[5] and intractable pediatric epileptic patients.[8] Thus, in the context of neuropathology the expanding OPC population could provide a viable source for neuronal replacement.

In the present study, our approach to the in vivo transdifferentiation of oligodendrocytes into neurons relied on two recent observations. First, Xue et al.[9] reported that suppression of polypyrimidine tract-binding (PTB) protein expression in cultured mouse embryonic fibroblasts caused 8% of the fibroblasts to differentiate into functional, NeuN-positive neurons. Although PTB protein expression impinges on the anti-neuronal RE-silencing transcription factor (REST)/SCP1 pathway,[10,11] the investigators found that suppression of the REST or SCP1 proved less effective compared to PTB protein suppression.[9] Thus, in vitro manipulation of PTB protein expression alone proved capable of inducing fibroblast-to-neuron reprogramming. Second, we recently developed a novel adeno-associated virus (AAV) vector where the chimeric capsid confers a dominant

Received 20 September 2016; accepted 11 January 2017;
http://dx.doi.org/10.1016/j.ymthe.2017.01.016.

Correspondence: Thomas J. McCown, UNC Gene Therapy Center, 5109 Thurston, CB 7352, Chapel Hill, NC 27599, USA.
E-mail: thomas_mccown@med.unc.edu

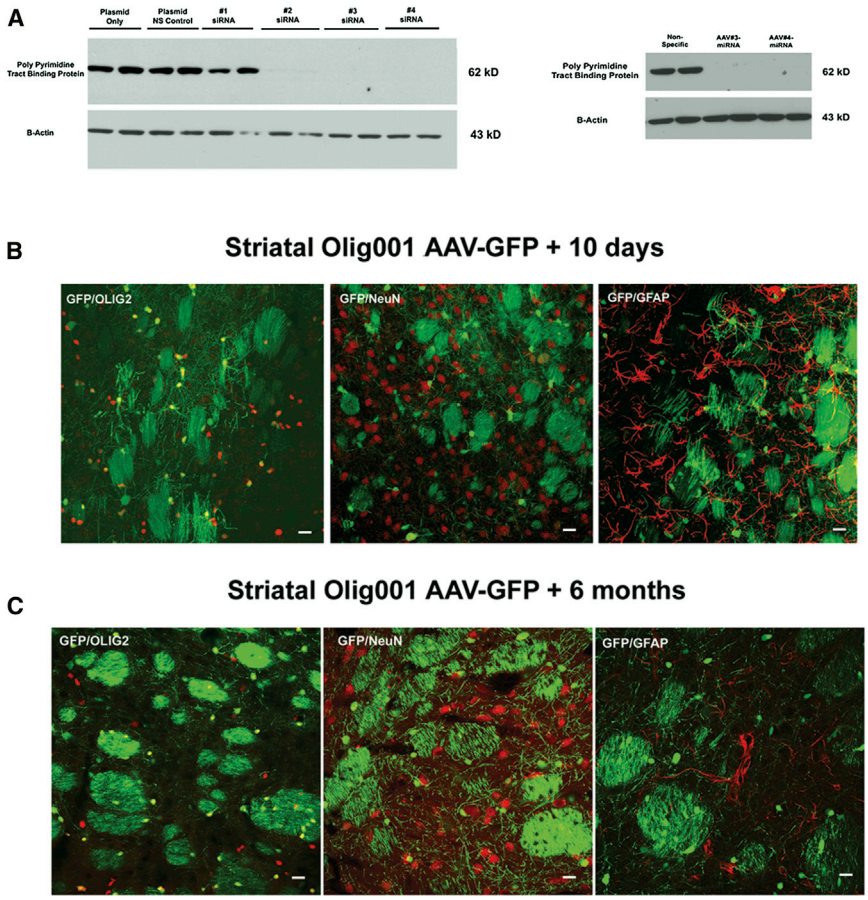

Figure 1. In Vitro Reduction of PTB Protein by siRNAs and miRNAs and Long-Term Selectivity of the Olig001 AAV Vector in the Rat Striatum

(A) The left western blot shows that siRNAs 3 and 4 completely prevented PTB protein expression following transfection of HeLa cells with the siRNA and a rat ptbp expression plasmid. The right western blot shows that conversion of siRNAs 3 and 4 into miRNAs 3 and 4, followed by packaging into recombinant AAV2 virus, prevents PTB protein expression in HEK293 cells. (B) The oligodendrocyte preference for the Olig001 AAV-GFP vector in the rat striatum 10 days post-transduction is shown. GFP-positive cells co-localized with Olig2-positive cells, but they did not co-localize with NeuN- or GFAP-positive cells. (C) The same transduction pattern from the Olig001 AAV-GFP vector 6 months after striatal transduction in the rat also is shown.

oligodendrocyte tropism in the rat striatum, even when gene expression is driven by a constitutive promoter.[12] Thus, this study tested whether long-term, cell-specific suppression of PTB protein expression in striatal oligodendrocytes could evoke a subsequent reprogramming of the transduced oligodendrocytes into functional neurons.

RESULTS

Initially, we identified two small interfering RNAs (siRNAs 3 and 4) that significantly inhibited PTB protein expression in HeLa cells (Figure 1A), and then we converted these siRNA sequences into microRNAs (miRNAs) using the BLOCK-iT Pol II miRNAi expression vector kit. Subsequently, miRNA-GFP constructs 3 and 4 were subcloned into an AAV plasmid where the gene expression is driven by a hybrid chicken beta-actin promoter. Recombinant AAV serotype 2 viruses were produced with these miRNA-GFP constructs, and then they were used to transduce HEK293 cells in vitro. Western blots established that the recombinant virus-derived miRNA gene expression substantially reduced the expression of PTB protein (Figure 1A).

As previously noted, a key component to our reprogramming approach involves the ability to target preferentially oligodendrocytes in vivo where gene expression is driven by a constitutive promoter active in both oligodendrocytes and neurons. As seen in Figure 1B, after direct striatal injection, recombinant AAV-GFP vectors packaged with the novel oligotropic capsid (Olig001) almost exclusively transduced oligodendrocytes in the rat striatum. Ten days post-vector infusion, the GFP-positive cells exhibited the classic morphology of striatal oligodendroctyes, including the marked presence of GFP in striatal patches that were composed primarily of myelinated projection axons. Furthermore, the GFP-positive cells did not co-localize with NeuN, a marker of neurons, or GFAP, a marker of astrocytes, but numerous cells did co-localize with Olig2, a marker of oligodendrocytes (Figure 1B). Also, this novel vector did not transduce dividing cells in the striatum, because 5-bromo-2-deoxyuridine (BrdU) administration during the initial period of Olig001 AAV-GFP transduction resulted in a total absence of GFP co-localization with BrdU-labeled striatal cells 2 weeks later (Figure S1). Most importantly, this dominant oligodendrocyte transduction pattern remained stable over time, given that the same oligodendrocyte transduction pattern was observed 6 months post-transduction (Figure 1C). Thus, the combination of this novel AAV vector with a constitutive promoter provided the ability to express initially the PTB protein miRNA predominantly in striatal oligodendrocytes, but also subsequently in transdifferentiated cells.

Based on the in vitro results, the miRNA-GFP construct 4 was packaged into recombinant AAV vectors using the oligodendrocyte preferring capsid plasmid, and the recombinant virus (AAV4miRNA-GFP) was directly injected into the rat striatum. Ten days later the majority of GFP-positive cells exhibited oligodendrocyte morphology, including co-localization with the oligodendrocyte marker Olig2, a lack of co-localization with the neuronal marker NeuN, and a substantial GFP presence in striatal patches (Figure 2A). However, by 6 weeks post-transduction, these transduced oligodendrocytes transdifferentiated into site-appropriate

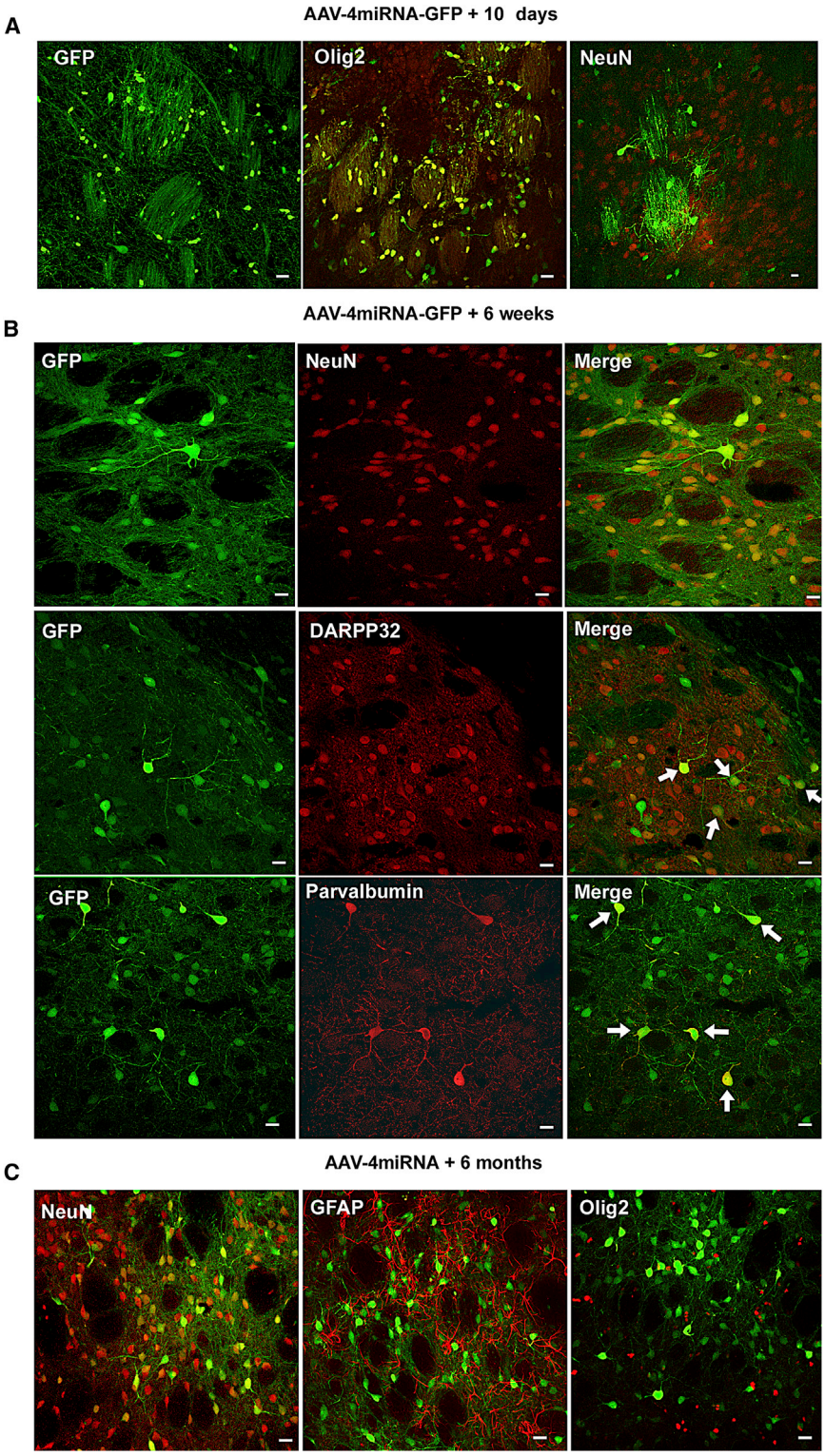

Figure 2. The Progression of Oligodendrocyte Transdifferentiation following Olig001 Packaged AAV4miRNA-GFP Transduction in the Rat Striatum

(A) Confocal images show that, 10 days after AAV4-miRNA-GFP transduction, the vast majority of the GFP-positive cells exhibit a typical oligodendrocyte morphology, including GFP-positive myelin in the striatal patches. Many GFP-positive cells co-localize with olig2, but they do not co-localize with NeuN. This pattern was present throughout the area of striatal transduction in all animals (n = 4). (B) By 6 weeks post-transduction, confocal images show that most of the GFP-positive cells co-localize with NeuN as well as subclasses of striatal GABAergic cells, such as DARPP32- and parvalbumin-positive neurons (arrows). NeuN/GFP co-localization was present throughout the area of transduction in all animals (n = 5). (C) Confocal images show that this neuronal pattern remains 6 months after vector transduction, where GFP-positive cells co-localize with NeuN, but not GFAP or Olig2 (n = 4). Scale bars, 20 μm.

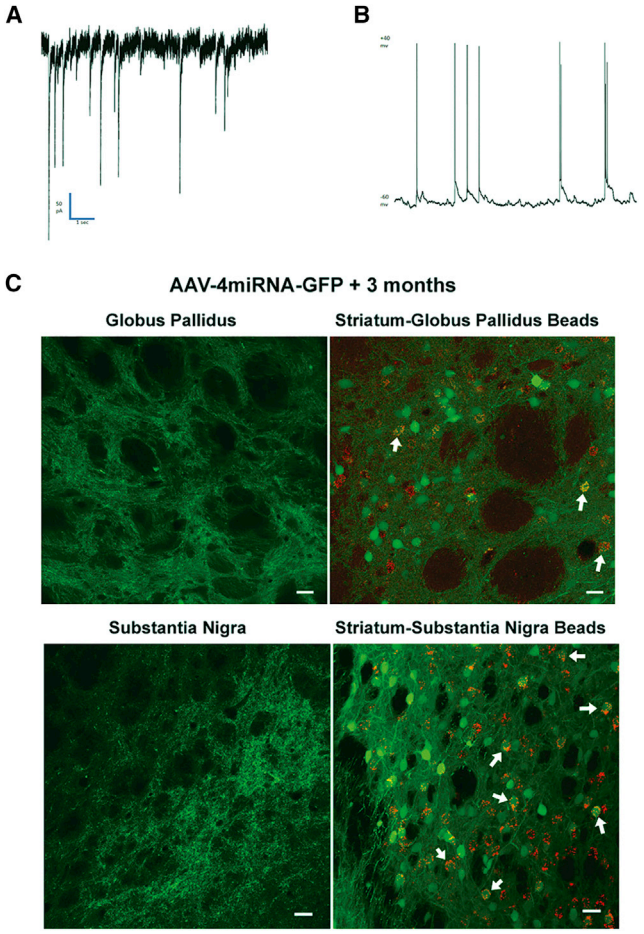

Figure 3. Electrophysiological and Neuroanatomical Evidence that the Transdifferentiated Oligodendrocytes Become Functional Striatal Neurons

(A) A voltage-clamp recording from a representative GFP-fluorescent striatal cell shows action potentials typical of a neuron. (B) A current-clamp recording shows spontaneous postsynaptic potentials from the cell in (A), indicative of synaptic input to the GFP-positive cell. (C) Confocal images show that, 3 months after AAV4miRNA-GFP transduction, GFP-positive nerve terminals are present in both the globus pallidus and the substantia nigra. Further, when fluorescent latex beads (0.04 μm) are infused into either the globus pallidus or substantia nigra 3 months after striatal transduction by AAV4miRNA-GFP, 2 weeks later the fluorescent beads have been retrogradely transported into GFP-positive cell bodies in the ipsilateral striatum (white arrows). Scale bars, 20 μm.

striatal neurons. As seen in Figure 2B, by 6 weeks post-transduction, the majority of the GFP-positive cells exhibited the typical morphology of striatal neurons, where the GFP co-localized with NeuN. Also, there was a marked absence of GFP in the striatal patches, and some of the GFP-positive cells co-localized with either DARRP32 or parvalbumin, both markers for subclasses of GABAergic striatal neurons (Figure 2B). Furthermore, a substantial population of GFP-positive neurons remained 6 months post-striatal transduction, with little evidence of GFP-positive oligodendrocytes (Figure 2C).

Although these reprogrammed oligodendrocytes exhibited many morphological and immunohistochemical properties indicative of striatal neurons, the question remained, were these cells functional neurons? To address this question, patch-clamp recordings were obtained from striatal slices either 6 weeks (three cells) or 3 months (three cells) post-AAV4miRNA-GFP transduction. Action potentials were recorded from six of six GFP-positive cells where these action potentials occurred spontaneously in four of six cells during voltage clamp at −60 mV (Figure 3A) and in four of five during current clamp. In the two cells that did not exhibit spontaneous action potentials, action potentials were elicited by a 300-ms current injection. Spontaneous postsynaptic currents were observed in five of six cells examined (Figure 3B). These spontaneous postsynaptic currents indicate that the recorded neurons were responding to neuronal inputs. Resting potential values were determined in five of the six neurons and ranged from a low of −26 mV to a high of −71 mV, with a mean of −47.6 mV.

Further functional validation included the presence of GFP-positive presynaptic terminals in two areas of striatal projection, the globus pallidus and the substantia nigra. Normally, striatal transduction with the Olig001 AAV-GFP vector does not result in GFP-positive terminals in the globus pallidus or substantia nigra (data not shown). However, 3 months after striatal transduction by the AAV4miRNA-GFP vectors, confocal microscopy revealed ipsilateral GFP-positive axon terminals in the globus pallidus and the substantia nigra (Figure 3C). To test the functional nature of these terminals, 0.04 μm fluorescent beads were infused into either the globus pallidus or the substantia nigra, 3 months after striatal AAV4miRNA-GFP vector administration. Then 2 weeks later the rats were sacrificed, and the presence of fluorescent beads in GFP-positive striatal cells was determined by confocal microscopy. A number of GFP-positive striatal cells contained the fluorescent beads following either globus pallidus or substantia nigra bead administration (Figure 3C). Thus, the GFP-positive presynaptic terminals proved capable of internalizing the fluorescent beads and retrogradely transporting the beads back to the striatal cell body. The presence of this retrograde axonal transport indicates functional presynaptic terminals.

DISCUSSION

The present study demonstrates that a single, non-toxic AAV vector can reprogram striatal oligodendrocytes, such that they transdifferentiate into functional neurons. Olig001 capsid AAV4miRNA-GFP-transduced striatal cells initially exhibited morphological and immunohistochemical properties unique to oligodendrocytes, similar to striatal transduction by control Olig001 capsid AAV-GFP vectors. However, in marked contrast to control Olig001 capsid AAV-GFP vectors, by 6 weeks post-treatment the transduced cells exhibited morphological, immunhistochemical, and electrophysiological properties unique to mature striatal neurons. Since Olig001 AAV-GFP-transduced cells did not co-localize with BrdU-labeled cells, this transition was not due to a differentiation of dividing progenitor cells. Furthermore, many of the transdifferentiated neurons expressed cellular markers indicative of subclasses of striatal neurons, so it is

likely that the striatal milieu exerts a significant influence on the fate of the transdifferentiated cells. Also, the occurrence of inhibitory postsynaptic currents indicates that these transdifferentiated neurons have integrated into the local circuitry, while the presence of distal axonal projections and functional retrograde transport suggest some level of structure-appropriate, distal integration. These measures strongly support the presence of functional transdifferentiated neurons. However, future studies must determine if these newly generated neurons exert significant influences on normal or pathological striatal function.

A crucial element to this neuronal replacement strategy involved the ability to express the gene product over the course of the initial transduction, as well as in the subsequent transdifferentiated cell. The vast majority of AAV serotypes exhibit a predominant neuronal tropism,[13,14] when gene expression is driven by a constitutive promoter. However, previous studies have shown that AAV8 or AAV1/2 serotypes can selectively support in vivo oligodendrocyte gene expression, but this oligodendrocyte tropism requires the use of oligodendrocyte-specific promoters, such as myelin basic protein.[15,16] Because the oligodendrocyte-specific promoter is not active in a neuron, as the oligodendrocyte transdifferentiates into a mature neuron, the resumption of PTB protein expression likely would reprogram the transdifferentiated neuron back to an oligodendrocyte or a cellular intermediate. By employing the Olig001 capsid AAV vector and a constitutive promoter, striatal gene expression was driven both in the initial transduced oligodendrocytes and in the subsequent transdifferentiated neurons. Certainly, this long-term PTB protein repression proved effective, as evidenced by the presence of transdifferentiated neurons 6 months post-transduction.

Another property of this vector-derived in vivo transdifferentiation involves the overall relative efficacy. By 6 weeks post-transduction, substantial numbers of the GFP-positive cells in the striatum exhibit neuronal properties with very few remaining GFP-positive oligodendrocytes or GFP-labeled striatal patches. In comparison, lentiviral-mediated suppression of PTB protein expression achieved an 8%–15% efficacy for in vitro embryonic fibroblast reprogramming,[9,17] while retroviral expression of ND4 and Insm1 induced 40% of cultured astrocytes to differentiate into neuronal-like cells.[18] One possible explanation for these differences could be the fact that our viral vector approach selectively targets endogenous cells within the CNS. However, a significant problem arises if the majority of the transdifferentiated cells arose from mature myelinating oligodendrocytes. Certainly, as seen in Figure 2, the transition to a neuronal phenotype was accompanied by a marked loss of GFP in the myelinated striatal patches. Such a loss of myelin could have adverse functional consequences. Therefore, future studies will focus on developing novel AAV vectors that selectively target oligodendrocyte progenitor cells, not mature myelinating oligodendrocytes. In summary, this viral vector-based transdifferentiation of resident oligodendrocytes provides a potential long-term neuronal replacement platform for both basic and therapeutic research.

MATERIALS AND METHODS

siRNA and Expression Plasmid Co-transfection

We tested four unique siRNAs and a non-targeting control siRNA (Thermo Scientific ON-TARGETplus Rat *ptbp1* gene). The *ptbp1* siRNA sequences were as follows: (1) CGGCAUCGUCCCAGA CAUA, (2) CAAUGGCGGUGUGGUCAAA, (3) CAACUUGAA CCCUGAGAGA, and (4) CCAACACUAUGGUUAACUA. We co-transfected the siRNA with a CMV promoter-containing, DDK-tagged rat *ptbp1* expression plasmid (OriGene) into HeLa cells in accordance with published Lipofectamine 2000 plasmid/siRNA co-transfection protocols (Life Technologies). The siRNA was resuspended in siRNA buffer (Thermo Scientific). Transfection was performed into 80%-confluent 12-well plates, with a volume of 1 mL antibiotic-free media. A total of 200 ng plasmid DNA and 20 pmol double-stranded RNA (dsRNA) was mixed with 100 μL optimum and 4 μL Lipofectamine 2000 and added to each well.

miRNA Plasmid Production

The BLOCK-iT Pol II miRNAi expression vector kit (Invitrogen) was used to prepare RNA polymerase II (Pol II)-based miRNA from the successful siRNA constructs. In accordance with kit instructions, miRNA primers were designed based on the two most successful siRNA sequences (siRNAs 3 and 4). Sequences designed to match PTBP1 siRNAs 3 and 4 were as follows: siRNA 3, top: TGCTGTCTCT CAGGGTTCAA GTTGCTGTTT TGGCCACTGA CTGACAGCAA CTTACCCTGA GAGA, bottom: CCTGTCTCTC AGGGTAAGTT GCTGTCAGTC AGTGGCCAAA ACAGCAA CTT GAACCCTGAG AGAC; and siRNA 4, top: TGCTGTAGTT AACCATAGTG TTGGCAGTTT TGGCCACTGA CTGACTGCCA ACAATGGTTA ACTA, bottom: CCTGTAGTTA ACCATTGTTG GCAGTCAGTC AGTGGCCAAA ACTGCCAACA CTATGGTTAA CTAC. Primers were prepared by Integrated DNA Technologies. Primers were annealed and ligated with pre-cut pcDNA 6.2-EmGFP plasmid per the manufacturer's instructions. Using high-fidelity PCR (Phusion, New England Biotechnologies), we amplified sequences for the non-specific miRNA (included with the BLOCK-iT kit) and PTBP1 miRNAs 3 and 4, along with their 5′ and 3′ miR flanking regions from the pcDNA 6.2-EmGFP plasmid, using primers containing a short overhang and a Not-1 restriction sequence (forward, agctgcggcc gcagggaggt agtgagtcgac; and reverse, tcatgcggcc gcgaaagctg ggtctagatatc). Amplified products were gel purified, digested with Not-1 restriction enzyme (New England Biolabs), and ligated immediately after the stop codon of EGFP in the plasmid TR-CBA-EGFP. Plasmid sequences were verified using a primer within the EGFP sequence (cgacaaccac tacctgagc).

Virus Production

The virus was produced in HEK293 cells as previously described.[19] Briefly, polyethylenimine max (PEI) was used for the triple transfection of the pXR2 or pOligO001 cap and rep plasmids, the pXX6-80 helper plasmid, and the TR-EGFP plasmid containing the nonspecific miRNA, or ptbp1 miRNA-3 or miRNA-4 flanked by inverted terminal repeats under the chicken beta-actin (CBA) promoter. Cells were

harvested between 48 and 72 hr post-transfection, and the virus was purified by cesium chloride ultracentrifugation. After identifying peak fractions by qPCR, the virus was dialyzed into PBS. Titers were calculated by qPCR according to established procedures using a LightCycler 480 instrument and SV40pA primers.[19]

Transduction/Transfection Verification of miRNA

rAAV2-packaged EGFP-miRNA virus was delivered at 1×10^5 MOI to HEK293 cells immediately upon splitting onto 12-well plates (2×10^5 cells per well). Then 24 hr post-transduction, 100 ng rat ptbp1 expression plasmid was transfected into cells using PEI (0.8 in 5 μL serum-free RPMI medium).

Electrophoresis and Western Blot

For both siRNA and AAV2/miRNA knockdown studies, 48 hr post-transfection cells were harvested by washing in ice-cold PBS and lysed in a buffer containing 150 mM NaCl, 50 mM Tris-HCl (pH 8), 0.1% NP40, 50 mM NaF, 30 mM β-glycerophosphate, 1 mM Na_3VO_4, and 1× Complete Protease Inhibitor cocktail (Roche). Equal amounts of proteins were electrophoresed on a 10% SDS-PAGE denaturing gel, followed by transfer onto a Hybond-ECL nitrocellulose membrane (GE Healthcare). The membrane was blocked with 5% fat-free powdered milk for 1 hr at room temperature, followed by overnight incubation at 4°C in anti-DDK (OriGene) in 5% BSA. Tubulin (Cell Signaling Technology) was used as a loading control. After washing, the membranes were incubated with anti-rabbit IgG-HRP. Bands were visualized by chemiluminescence.

Animals and Stereotactic Infusions

All of the animals were male Sprague-Dawley rats (Charles River Laboratories) weighing ~300 g at the time of intracranial injection. The animals were maintained on a 12-hr light-dark cycle and had free access to water and food. For all animal studies, care and procedures were in accordance with the NIH Guide for the Care and Use of Laboratory Animals, and all procedures received prior approval by the University of North Carolina Institutional Animal Care and Usage Committee.

Virus vector infusions were performed as previously described.[20] First, animals were anesthetized with 50 mg/kg pentobarbital and placed into a stereotactic frame. Using a 32G stainless steel injector and a Sage infusion pump, animals received 2 μl unilaterally of either Olig001 packaged AAV-GFP or Olig001 packaged AAV4miRNA-GFP over 10 min into the striatum (0.5 mm anterior to bregma, 3.5 mm lateral, and 5.5 mm vertical, according to the atlas of Paxinos and Watson).[21] The injector was left in place for 3 min post-infusion in order to allow diffusion from the injector. For the fluorescent bead injections, 3 months after the striatal 4miRNA virus infusion, rats (n = 3) were anesthetized and placed into the stereotactic frame. Subsequently, fluorescent latex beads (0.5 μL/5 min, Fluospheres 580/605, 1:5 dilution, Molecular Probes, Millipore) were infused into the globus pallidus (1.0 mm posterior to bregma, 3.0 mm lateral, and 7.0 mm vertical) or the substantia nigra (5.3 mm posterior to bregma, 2.5 mm lateral, and 8.0 mm vertical). The injector was left in place for 3 min post-infusion in order to allow diffusion from the injector. Finally, for the BrdU study, rats (n = 2) received 100 mg/kg 5-bromo-2-deoxyuridine intraperitoneally (i.p.) (Sigma) 30 min prior to the Olig001 AAV-GFP virus injection into the striatum as described above. A second 100 mg/kg dose of BrdU was administered 30 min post-virus injection in order to ensure labeling of dividing cells during the initial period of virus infection.

Immunohistochemistry and Confocal Microscopy

Ten days, 6 weeks, 3 months, or 6 months after the vector infusion, animals received an overdose of pentobarbital (100 mg/kg pentobarbital i.p.), and they were perfused transcardially with ice-cold 100 mM sodium PBS (pH 7.4), followed by 4% paraformaldehyde in PB (pH 7.4). After brains were post-fixed 12–48 hr at 4°C in the paraformaldehyde-PB, 40-μm coronal sections were cut using a vibrating blade microtome for subsequent immunofluorescence. For the BrdU study only, initially the sections were incubated in 1 N HCl at 63°C for 3 min. Then for all of the conditions, the sections were washed three times in PBS and blocked in 10% goat serum/PBS for 45 min. To determine GFP cellular co-localization, tissue sections were incubated in the blocking solution with one of the following antibody cellular markers: NeuN (1:500, Chemicon), GFAP (1:2,000, Dako), Olig2 (1:500, Millipore), DARPP32 (1:500, Abcam), or parvalbumin (1:500, Millipore). The BrdU study utilized a primary BrdU antibody (1:200, Millipore). Following incubation at 4°C for 48–72 hr in primary antibodies, the sections were rinsed three times with PBS and blocked again for 45 min at room temperature. Subsequently, the tissue sections were incubated in either Alexafluor 594-conjugated goat anti-rabbit IgG or goat anti-mouse (1:500, Invitrogen) for 1 hr at 4°C. Rinsed sections were mounted, and fluorescence was visualized using a Zeiss LM 780 confocal microscope in the UNC Neuroscience Center Confocal and Multiphoton Imaging Core. GFP co-localization was determined on the z axis.

Patch-Clamp Electrophysiology

Electrophysiological recordings were obtained from GFP-fluorescent cells in both current-clamp and voltage-clamp modes using standard electrophysiological techniques.[22] Briefly, 300-μm coronal vibrotome sections were cut in oxygenated (95% O_2/5% CO_2) ice-cold, bicarbonate-buffered artificial cerebrospinal fluid (ACSF). After a 1-hr incubation in that ACSF at room temperature (22°C), samples were transferred to a flow chamber containing room temperature ACSF. Whole-cell patch recordings were obtained from fluorescent cells using a high Cl^- internal solution as previously described.[14] Neurons were clamped to −60 mV for voltage-clamp recording and either maintained at their normal resting potential or forced to −60 mV by current injection for current-clamp recording. Brief (300-ms) current injections were administered during voltage clamp for some cells to elicit an action potential.

SUPPLEMENTAL INFORMATION

Supplemental Information includes one figure and can be found with this article online at http://dx.doi.org/10.1016/j.ymthe.2017.01.016.

AUTHOR CONTRIBUTIONS

M.S.W. constructed the miRNAs and made the recombinant AAV2 and Olig001 AAV miRNA viruses. A.B. performed the western blots. H.E.C. performed the in vitro electrophysiological experiments. S.K.P. made the Olig001 GFP viruses. T.J.M. designed the research, performed all other experiments, analyzed the data, and wrote the manuscript.

CONFLICTS OF INTEREST

M.S.W. and T.J.M. are named as inventors on a patent filed by UNC for oligodendrocyte-to-neuron reprogramming. The remaining authors declare no conflicts of interest.

ACKNOWLEDGMENTS

These studies were supported by a Target ALS grant (T.J.M.) and NINDS grant NS082289 (T.J.M.). Confocal microscopy was conducted in the UNC Neuroscience Center Confocal and Multiphoton Imaging Core (NINDS center grant P30 NS045892).

REFERENCES

1. Heinrich, C., Spagnoli, F.M., and Berninger, B. (2015). In vivo reprogramming for tissue repair. Nat. Cell Biol. *17*, 204–211.
2. Guo, Z., Zhang, L., Wu, Z., Chen, Y., Wang, F., and Chen, G. (2014). In vivo direct reprogramming of reactive glial cells into functional neurons after brain injury and in an Alzheimer's disease model. Cell Stem Cell *14*, 188–202.
3. Torper, O., Pfisterer, U., Wolf, D.A., Pereira, M., Lau, S., Jakobsson, J., Björklund, A., Grealish, S., and Parmar, M. (2013). Generation of induced neurons via direct conversion in vivo. Proc. Natl. Acad. Sci. USA *110*, 7038–7043.
4. Heinrich, C., Bergami, M., Gascón, S., Lepier, A., Viganò, F., Dimou, L., Sutor, B., Berninger, B., and Götz, M. (2014). Sox2-mediated conversion of NG2 glia into induced neurons in the injured adult cerebral cortex. Stem Cell Reports *3*, 1000–1014.
5. Kang, S.H., Li, Y., Fukaya, M., Lorenzini, I., Cleveland, D.W., Ostrow, L.W., Rothstein, J.D., and Bergles, D.E. (2013). Degeneration and impaired regeneration of gray matter oligodendrocytes in amyotrophic lateral sclerosis. Nat. Neurosci. *16*, 571–579.
6. Luo, Y., Hu, Q., Zhang, Q., Hong, S., Tang, X., Cheng, L., and Jiang, L. (2015). Alterations in hippocampal myelin and oligodendrocyte precursor cells during epileptogenesis. Brain Res. *1627*, 154–164.
7. Joseph, M.J., Caliaperumal, J., and Schlichter, L.C. (2016). After intracerebral hemorrhage, oligodendrocyte precursors proliferate and differentiate inside white-matter tracts in the rat striatum. Transl. Stroke Res. *7*, 192–208.
8. Sakuma, S., Halliday, W.C., Nomura, R., Ochi, A., and Otsubo, H. (2014). Increased population of oligodendroglia-like cells in pediatric intractable epilepsy. Neurosci. Lett. *566*, 188–193.
9. Xue, Y., Ouyang, K., Huang, J., Zhou, Y., Ouyang, H., Li, H., Wang, G., Wu, Q., Wei, C., Bi, Y., et al. (2013). Direct conversion of fibroblasts to neurons by reprogramming PTB-regulated microRNA circuits. Cell *152*, 82–96.
10. Ballas, N., Grunseich, C., Lu, D.D., Speh, J.C., and Mandel, G. (2005). REST and its corepressors mediate plasticity of neuronal gene chromatin throughout neurogenesis. Cell *121*, 645–657.
11. Conaco, C., Otto, S., Han, J.J., and Mandel, G. (2006). Reciprocal actions of REST and a microRNA promote neuronal identity. Proc. Natl. Acad. Sci. USA *103*, 2422–2427.
12. Powell, S.K., Khan, N., Parker, C.L., Samulski, R.J., Matsushima, G., Gray, S.J., and McCown, T.J. (2016). Characterization of a novel adeno-associated viral vector with preferential oligodendrocyte tropism. Gene Ther. *23*, 807–814.
13. Burger, C., Gorbatyuk, O.S., Velardo, M.J., Peden, C.S., Williams, P., Zolotukhin, S., Reier, P.J., Mandel, R.J., and Muzyczka, N. (2004). Recombinant AAV viral vectors pseudotyped with viral capsids from serotypes 1, 2, and 5 display differential efficiency and cell tropism after delivery to different regions of the central nervous system. Mol. Ther. *10*, 302–317.
14. Cearley, C.N., and Wolfe, J.H. (2006). Transduction characteristics of adeno-associated virus vectors expressing cap serotypes 7, 8, 9, and Rh10 in the mouse brain. Mol. Ther. *13*, 528–537.
15. Lawlor, P.A., Bland, R.J., Mouravlev, A., Young, D., and During, M.J. (2009). Efficient gene delivery and selective transduction of glial cells in the mammalian brain by AAV serotypes isolated from nonhuman primates. Mol. Ther. *17*, 1692–1702.
16. von Jonquieres, G., Fröhlich, D., Klugmann, C.B., Wen, X., Harasta, A.E., Ramkumar, R., Spencer, Z.H., Housley, G.D., and Klugmann, M. (2016). Recombinant human myelin-associated glycoprotein promoter drives selective AAV-mediated transgene expression in oligodendrocytes. Front. Mol. Neurosci. *9*, 13.
17. Xue, Y., Qian, H., Hu, J., Zhou, B., Zhou, Y., Hu, X., Karakhanyan, A., Pang, Z., and Fu, X.D. (2016). Sequential regulatory loops as key gatekeepers for neuronal reprogramming in human cells. Nat. Neurosci. *19*, 807–815.
18. Masserdotti, G., Gillotin, S., Sutor, B., Drechsel, D., Irmler, M., Jørgensen, H.F., Sass, S., Theis, F.J., Beckers, J., Berninger, B., et al. (2015). Transcriptional mechanisms of proneural factors and REST in regulating neuronal reprogramming of astrocytes. Cell Stem Cell *17*, 74–88.
19. Grieger, J.C., Choi, V.W., and Samulski, R.J. (2006). Production and characterization of adeno-associated viral vectors. Nat. Protoc. *1*, 1412–1428.
20. Haberman, R.P., Samulski, R.J., and McCown, T.J. (2003). Attenuation of seizures and neuronal death by adeno-associated virus vector galanin expression and secretion. Nat. Med. *9*, 1076–1080.
21. Paxinos, G., and Watson, C. (1998). The Rat Brain in Stereotaxic Coordinates, Fourth Edition (New York: Academic Press).
22. Ming, Z., Criswell, H.E., Yu, G., and Breese, G.R. (2006). Competing presynaptic and postsynaptic effects of ethanol on cerebellar purkinje neurons. Alcohol. Clin. Exp. Res. *30*, 1400–1407.